Comparison of Two and Three-Dimensional Optical Tomographic Image Reconstructions of Human Finger Joints

Rong Song, Alexander D. Klose, Alexander K. Scheel, Uwe Netz, Jürgen Beuthan, Andreas H. Hielscher

***Abstract* — We have developed an image reconstruction algorithm to recover the spatial distribution of optical properties in human finger joints for early diagnosis and monitoring of rheumatoid arthritis (RA). An optimization method iteratively employs a light propagation model based on the equation of radiative transfer (ERT) for recovering the unknown absorption and scattering coefficients distribution for near-infrared (NIR) light inside the joint tissue. We explored the differences in cross-sectional images obtained by using the reconstruction algorithms with 2-dimensional and 3-dimensional light propagation models. In particular we examined how these different approaches affect the discrimination between healthy and RA joints.**

I. Introduction

In previous studies we have demonstrated the applications of two-dimensional (2D) sagittal tomographic imaging of human proximal interphalangeal (PIP) joints using the equation of radiative transfer (ERT) as light propagation model [1,2]. To further improve on the promising clinical results and to potentially increase sensitivity and specificity, we have developed an algorithm that employs a three-dimensional (3D) model of light propagation. In addition, we implemented an image evaluation scheme to further quantify individual reconstructed images and to better classify the differences between healthy joints and joints affected by RA. Image reconstruction results based on the algorithms that employ 2D and 3D models are compared and evaluated with respect to clinical utility for optical RA diagnostics.

This work was supported in part by a grant from the National Institute of Arthritis Musculosceletal and Skin Diseases (NIAMS-R01-AR046255) at the National Institutes of Health.

Rong Song, Alexander D. Klose, and Andreas H. Hielscher are with the Depts. of Biomedical Engineering and Radiology at Columbia University, New York, NY 10027 USA (phone: 212-854-5080; fax:212-854-8725; e-mail: ahh2004@columbia.edu).

A. K. Scheel is with the Abteilung für Nephrologie und Rheumatologie, Georg-August-Universität Göttingen, 37075 Göttingen, Germany.

U. J. Netz and J. Beuthan are with the Institut für Medizinische Physik und Lasermedizin, Charité – Universitätsmedizin Berlin, 14195 Berlin, Germany.

II. Methods

A. Data Acquisition

The measurement data were collected from PIP joints with a joint imaging system as introduced by Hielscher et al [1]. Fig. 1 shows some details of the set up. A human finger is placed

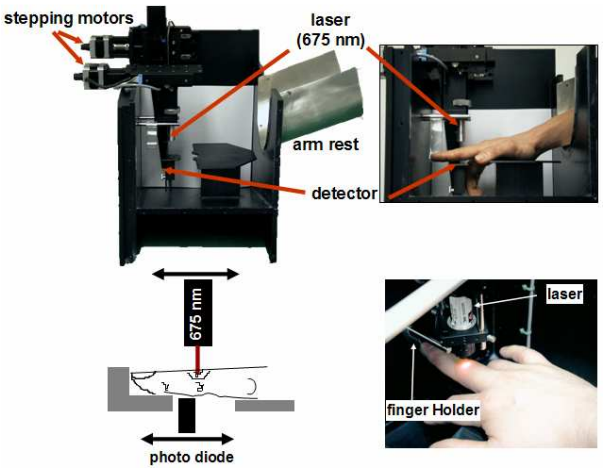

Fig. 1. Experimental setup of finger reconstruction

inside the equipment between a laser diode and detector. A laser diode illuminates the finger (dorsal side) at 11 different points with a spatial separation of 0.2 cm. A silicon diode measured the transmitted light on the palmar side of the joint at 16 different positions with a spatial separation of 0.2cm. The measurement time is approximately 3 minutes. In addition, a physician determines finger thickness at 3 different points. Using measurement data and finger thickness values we then set up the 2D and 3D fingers models and perform image reconstructions accordingly.

B. Image Reconstruction

We employ a nonlinear optimization approach to reconstruct the unknown distribution of optical parameters (absorption coefficient μ_a and scattering coefficient μ_s) inside the tissue [3]. This approach requires 3 elements. First a forward model for light transport in tissue predicts the detector readings on the tissue boundary for a given initial distribution of μ_a and μ_s. Using an objective function, the differences between the predicted detector readings and actual measurements are quantified. Typically the objective function φ is defined as the χ^2-error norm of the predicted and measured detector readings plus some additional regularization terms if needed. In the third step, this objective function is minimized by iteratively updating the initial optical parameter distribution along an appropriately selected search direction. The optimization process is finished after the measured and predicted data match, i.e. a minimum of the objective function is found and the final distribution of μ_a or μ_s is displayed in an image.

The light distribution originating from a source positioned at the outer boundary of a finger joint can be described most accurately by the equation of radiative transfer (ERT). Using a time-independent formulation this equation can be written as

$$\Omega \bullet \nabla \psi + (\mu_a + \mu_s)\psi = \mu_S \int_{4\pi} p(\Omega,\Omega')\psi(\Omega')d\Omega' \qquad (1)$$

Here, ψ *(**r**,* Ω *)* is the radiance at spatial position ***r*** and direction Ω .The scattering phase function $p(\Omega, \Omega')$ is described by the Henyey-Greenstein function and takes the anisotropic scattering behavior of biological tissue into account. The boundary condition for the ERT consists of partially reflected light, due to the refractive index mismatch, and of boundary sources $S(\boldsymbol{\Omega}, \boldsymbol{r})$ at $\boldsymbol{r} \in \partial V$. It is given by

$$\psi(r,\Omega) = S(r,\Omega) + R(|\Omega' \bullet n|)\psi(r,\Omega') \qquad (2)$$

for all $n \cdot \Omega < 0$ at ∂V. The direction Ω' points outward $\Omega' = \Omega - 2(\Omega \cdot n)n$ for all $n \cdot \Omega' > 0$ at ∂V . The reflectivity R is given with

$$R(\cos\vartheta') = \frac{1}{2}\left(\frac{n_m \cos\vartheta'' - n_0 \cos\vartheta'}{n_m \cos\vartheta'' + n_0 \cos\vartheta'}\right)^2 + \frac{1}{2}\left(\frac{n_m \cos\vartheta' - n_0 \cos\vartheta''}{n_m \cos\vartheta' + n_0 \cos\vartheta''}\right)^2 \qquad (3)$$

where the angle of incidence ϑ' from within the medium with refractive index n_m is given by $\cos\vartheta' = \Omega' \cdot n$. The refracted angle ϑ'' in the outside medium (air) with $n_0 = 1$ satisfies *Snell's* law $n_m \sin\vartheta' = n_0 \sin\vartheta''$. The critical angle ϑ'_c for total internal reflection is given by $n_m \sin\vartheta'_c = n_0$.

We solve the ERT with a *source iteration* method based on a *finite difference discrete-ordinates* discretization [3,4]. The direction Ω is replaced with a set of discrete ordinates Ω_k with full level symmetry. The spatial derivatives are substituted with finite difference approximations defined on a structured *Cartesian* grid.

The resulting system of equations is solved by a Gauss-Seidel method, where the in-scatter source term is updated at each source iteration. Numerically solving the 2D-ERT takes approximately 2-4 minutes, whereas a full 3D calculation requires 15-30 minutes.

The spatial distribution of the optical parameters is reconstructed by applying a limited-memory Broyden-Fletcher-Goldfarb-Shanno (BFGS) technique to an objective function $\varphi(\mu)$ that describes the difference between the measured, m_d, and predicted data, p_d. The predicted detector readings p_d at the boundary are derived from the numerical solution given by the partial current *J*. We minimize the objective function and the final result is the distribution of the optical parameters. The BFGS method requires the gradient of the objective function, $d\varphi/d\mu$, which is calculated by means of an adjoint differentiation technique. More details can be found, for example, in Klose et al [3].

The image reconstructions were performed either on a 2D or 3D Cartesian grid. The 2D Cartesian grid represented a saggital tissue slice through the center of the PIP joint. The tissue surface geometry was only modeled for the dorsal and palmar side of the finger. The 3D Cartesian grid represented the complete 3D tissue surface of the PIP joint. The tissue surface was simplified by a cylindrical model with elliptic cross-sections and a conical shape extending toward the finger tip. The finger reconstructions were performed on both grids using the same sets of measurement data. We studied the image reconstruction performance and expected that 3D reconstructions were qualitatively and quantitatively better than 2D reconstructions, on the expense of computational processing time.

C. *Image Analysis*

Using near-infrared light at wavelength = 678 nm, we have performed tomographic measurements on human PIP joints. We reconstructed μ_s and μ_a by using the measurement data and a Cartesian grid of a finger joint model with approximately 200,000 grid points. The number of grid points depends on the spatial discretization Δx, Δy and Δz and the actual physical dimensions of the finger. Typically, the reconstruction code requires four to five BFGS iterations before convergence, which can take between 30 hours and 3 days on a single 3.0 GHz Pentium IV processor. Fig. 2a shows a typical reconstruction result. In the center of the image a region with low absorption (scattering) is visible, which is indicative of the joint cavity. The joint cavity is filled with synovial fluid having very small absorption coefficients. This region is flanked by areas of higher absorption and scattering, typical for the cartilage and bone. To quantify the width of the central "dip," we compute the full width at half maximum (FWHM). By putting three horizontal lines across the reconstructed images, as shown in Fig. 2a, we determine the half-max μ_a distances along the proximal direction, which is shown in the Fig. 2b. The results can be further understood as computing the average dip area when we put more and more horizontal lines across the images.

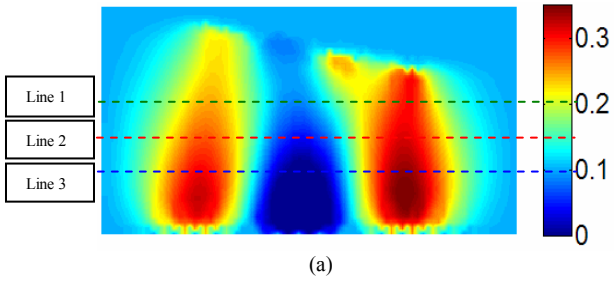

(a)

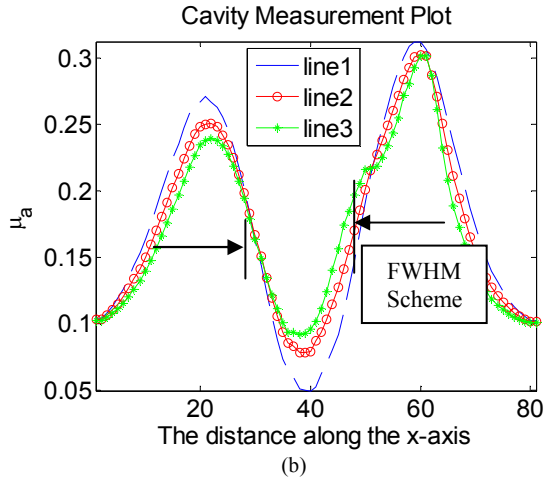

(b)

Fig. 2 Width measurement illustration for absorption image

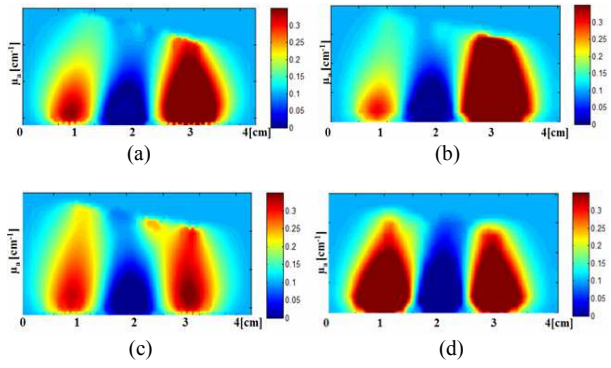

(a) (b) (c) (d)

Fig. 3. Two dimensional and three dimensional healthy joints reconstruction of μ_a

(a) (c) Two dimensional healthy joints reconstruction of μ_a

(b) (d) Central slice of three dimensional healthy joints reconstruction of μ_a with the finger of (a),(c) respectively

III. EXPERIMENTAL RESULTS

Figure 3 shows the μ_a distributions in a cross-section through the PIP joints of two healthy volunteers. Figures 3a and 3c were obtained using the 2D code, while figures 3b and 3d

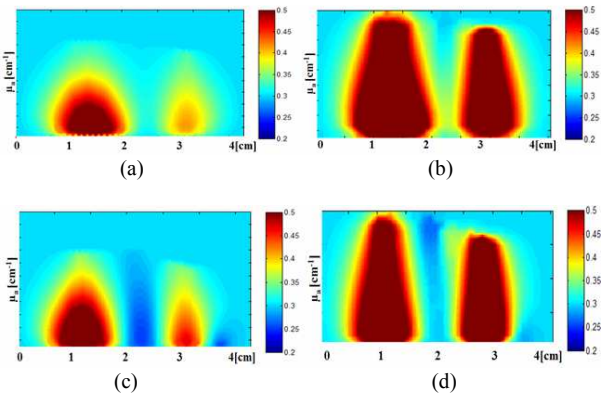

(a) (b) (c) (d)

Fig. 4. Two dimensional and three dimensional RA joints reconstruction of μ_a

(a) (c) Two dimensional RA joints reconstruction of μ_a

(b) (d) Central slice of three dimensional RA joints reconstruction of μ_a with the finger of (a),(c) respectively

were obtained using the 3D code. Similarly, Fig. 4 shows images from two patients with RA. We observed that the spatial distribution of μ_a slightly differs between images generated by the 2D and 3D models. For example, Fig. 3a and Fig. 3c show 2D reconstruction of absorption coefficient with the smallest value μ_a = 0.01 cm^{-1} inside the cavity. The adjacent tissue parts to the left and to the right in the image depict bones, which show absorption coefficient of approximately 0.3 cm^{-1} That is about 20 – 40% lower than

what we found by using a 3D reconstruction model, as shown in Fig. 3b and Fig. 3d. Similar observations can be made in the case of the RA patients, shown in Fig. 4.

By applying the measurement scheme we set up above, we can quantify the differences of cavity FWHM between 2D and 3D reconstructions. The results are μ_s listed in Table 1 and Table 2. We can see that the FWHM values obtained using the3D images are on average (see mean values in table) slightly wider than those obtained using the 2D model. This is true for healthy as well RA joints.

	Healthy Joints Cavity Width (mm) Number of fingers N=6		**RA Joints Cavity Width (mm)** Number of fingers N=7	
	2D	3D	2D	3D
MEAN	10.7500	11.8333	9.7619	9.8572
STD	0.2528	0.5055	1.4397	0.9786
95% Confidence Interval	[10.5477 10.9523]	[11.4288 12.2579]	[8.6954 10.8285]	[9.1322 10.5821]

Table 1: Full width at half maximum (FWHM) measurement

	2D	**3D**
p-value	0.15	0.001

Table 2: T-test comparison of 2D and 3D

Furthermore, we observed that within the joints with dip in optical tomographic images (early stages of RA), the joint width as seen in optical tomographic images are narrower than those in healthy volunteers. For example, Fig. 5a and Fig. 5b show healthy PIP joints reconstructions and Fig. 5c and

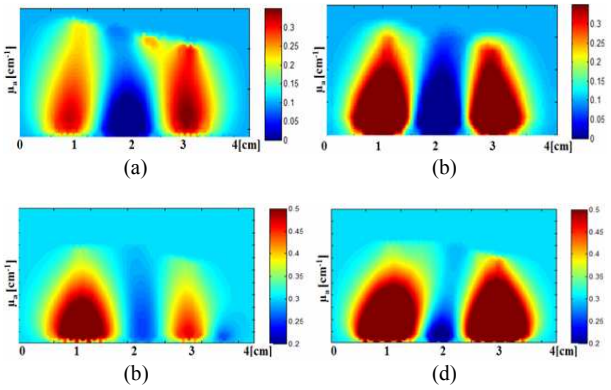

Fig. 5. Finger joints reconstruction of μ_a
(a)(b), healthy joints reconstruction of μ_a
(c)(d), RA joints reconstruction of μ_a

Fig. 5d show RA PIP joints reconstructions. In this case we can easily notice the differences in the width of the central dip. Comparing the mean FWHM values found in 3D reconstructions for healthy joints (11.8333mm) and joints affected by RA (9.8572mm), we find that this difference is statistically significant (p = 0.001, see Table 2). When instead of 3D reconstructions, 2D reconstructions are used to compare healthy and RA joints, the differences in FWHM values are not statistically significant (p = 0.15). These results underscore the necessity of using a 3D model in the reconstruction process.

In general, fingers affected with rheumatoid arthritis will show symptoms such as swelling, turbid synovial fluid, neo-vascularization and inflammation, and bone erosion (in later stages). All of these symptoms will lead to an increase of μ_a and μ_s values, which is confirmed by our observations.

IV. CONCLUSION

Based on our investigation, both 2D and 3D image reconstructions of same finger joints successfully show anticipated results, and both methods show an absorption and scattering "dip" in the location of joint cavity. However, we also observe that the spatial distribution of absorption and scattering is slightly different between images generated by the 2D and 3D models. 3D image reconstructions show higher bone absorptions than those by the 2D model and the width of the dips are different from 2D reconstruction results. Most importantly, only 3D reconstruction images show statistically significant differences between the width of joints of healthy patients and joints affected by RA. This finding underscores the necessity of full 3D reconstruction methods to increase the diagnostic value of optical tomographic methods

REFERENCES

[1] A H. Hielscher, A.D. Klose, A.K. Scheel, B. Moa-Anderson, M. Backhaus, U. Netz, J. Beuthan, "Sagittal laser optical tomography for imaging of rheumatoid finger joints," Phys. Med. Biol. 49, 1147-1163 (2004).

[2] A.K. Scheel, M. Backhaus, A.D. Klose, B. Moa-Anderson, U. Netz, K.G. Hermann, J. Beuthan, G. Muller, G.R. Burmester, A.H. Hielscher, "First clinical evaluation of sagittal laser optical tomography for detection of synovitis in arthritic finger joints," Annals of the Rheumatoic Diseases 64, 239-245 (2005).

[3] A. D. Klose and A. H. Hielscher, "The inverse source problem based on the radiative transfer equation in optical molecular imaging," Journal of Computational Physics 202, 323-345 (2005).

[4] B. G. Carlson and K. D. Lathrop, "Transport theory - The method of discrete ordinates," in: H. Greenspan et al. (Eds.), Computing Methods in Reactor Physics, Gordon and Breach, New York, pp. 166-266, 1968.